Two-particle correlations in continuum dipole transitions in Borromean nuclei

doi: 10.1103/PhysRevC.80.031301

PHYSICAL REVIEW C **80**, 031301(R) (2009)

Two-particle correlations in continuum dipole transitions in Borromean nuclei

K. Hagino,[1] H. Sagawa,[2] T. Nakamura,[3] and S. Shimoura[4]
[1]*Department of Physics, Tohoku University, Sendai 980-8578, Japan*
[2]*Center for Mathematical Sciences, University of Aizu, Aizu-Wakamatsu, Fukushima 965-8560, Japan*
[3]*Department of Physics, Tokyo Institute of Technology, 2-12-1 O-Okayama, Tokyo 152-8551, Japan*
[4]*Center for Nuclear Study, University of Tokyo (CNS) RIKEN Campus, 2-1 Hirosawa, Wako, Saitama 351-0198, Japan*
(Received 11 August 2009; published 14 September 2009)

We study the energy and angular distributions of two emitted neutrons from the dipole excitation of two typical, weakly bound Borromean nuclei, ^{11}Li and ^{6}He, by using a three-body model. Our calculation indicates that those distributions are considerably different between the two nuclei, even though both the nuclei exhibit similar strong dineutron correlations in the ground state to each other. We point out that this different behavior primarily reflects the interaction between the neutron and the core nucleus, especially the s-wave virtual state in ^{10}Li, rather than the interaction between the valence neutrons.

DOI: 10.1103/PhysRevC.80.031301 PACS number(s): 21.10.Gv, 23.20.−g, 25.60.Gc, 27.20.+n

Borromean nuclei are unique three-body bound systems, in which any two-body subsystem is not bound [1,2]. Typical examples include ^{11}Li and ^{6}He, which can be viewed as three-body systems consisting of a core nucleus and two valence neutrons. The binding energy of these neutron-rich nuclei is considerably small (the two-neutron separation energy, S_{2n}, is 378 keV [3] and 975 keV for ^{11}Li and ^{6}He, respectively, which can be compared with, e.g., $S_{2n} = 12.2$ MeV for ^{18}O), and a few intriguing features originating from the weakly bound property have been found. A halo structure, in which the density distribution of valence neutrons extends far beyond the core nucleus [4,5], and a strong low-energy electric dipole ($E1$) transition [6,7] are well-known examples.

One of the most important current open questions concerning the Borromean nuclei is to clarify the characteristic nature of correlations between the two valence neutrons, which do not form a bound state in the vacuum. A strong dineutron correlation, where the two neutrons take a spatially compact configuration, has been theoretically predicted for some time [1,5,8–10] (see also Refs. [11,12]). It has been, however, a difficult task to probe experimentally the dineutron correlation. In fact, it is only recently that the strong low-lying dipole strength distribution has been observed experimentally in the ^{11}Li nucleus, which strongly suggests the existence of dineutron correlation in this nucleus.

More direct information on the correlations in two-particle wave functions may be obtained by measuring the energy and angular distributions of two emitted neutrons [13–16]. Because neither ^{11}Li nor ^{6}He has a bound excited state, the Borromean nuclei must be broken up to a three-body continuum state once they are excited as a result of the interaction with another nucleus. Notice that the operator that induces the $E1$ excitation is proportional to the center of mass coordinate of the two valence neutrons, $\boldsymbol{R} = (\boldsymbol{r}_1 + \boldsymbol{r}_2)/2$ [8,17], where $\boldsymbol{r}_1$ and $\boldsymbol{r}_2$ are the coordinates for the two neutrons. Therefore, the relative motion of the two neutrons, $\boldsymbol{r} = \boldsymbol{r}_1 - \boldsymbol{r}_2$, is not affected by the $E1$ excitations at all. It is thus interesting to ask how the energy and angular distributions from the $E1$ excitation reflect the ground state correlations of the Borromean nuclei. By studying the two neutron correlations in the energy and angular distributions, one may also be able to shed some light on the Efimov effect [18], which is a general feature of a three-body system in which at least two of the three two-body subsystems have an infinite s-wave scattering length [19].

The aim of this article is to address this question theoretically using a three-body model for the Borromean nuclei. The model that we employ is the same as that in Refs. [9,20], that is, a three-body model with a density-dependent zero-range pairing interaction between the two neutrons. The model predicts similar strong dineutron correlations for both ^{11}Li and ^{6}He, although the main configurations of the ground states are different: the $[p_{1/2}]^2$ and $[s_{1/2}]^2$ configurations are strongly mixed in ^{11}Li, whereas the $[p_{3/2}]^2$ configuration is the major component in ^{6}He. It has been shown that the model has successfully reproduced the experimental $E1$ strength distribution for both the nuclei [6,21,22].

Because the basic formulas for the energy and angular distributions based on the three-body model are already given in Ref. [17], we do not repeat them here. For the neutron-neutron and the neutron-core interactions, we use exactly the same parameters as those in Ref. [9], except for the radius parameter for the density-dependent term in the pairing interaction for the ^{11}Li nucleus. We have slightly adjusted it so that the new empirical value of $S_{2n} = 378$ keV [3] is reproduced. This yields an s-wave probability of 20.6% in the ground state of ^{11}Li. To calculate the continuum response, we treat approximately the recoil kinetic energy of the core nucleus for the three-body final state of the dipole response, although it is treated exactly for the initial (ground) state (see Refs. [21,22] for details). The approximation works reasonably well for both ^{11}Li and ^{6}He, although the height of the peak is slightly underestimated for the ^{11}Li nucleus [21].

Figures 1 and 2 show the dipole strength distribution, $d^2B(E1)/de_1de_2$, as a function of the energies of the two emitted neutrons for the ^{11}Li and ^{6}He nuclei, respectively. Here, e_1 (e_2) is the relative energy between the first (second) neutron and the core nucleus. Notice that these energy distributions are symmetric with respect to the interchange of e_1 and e_2. Figure 1(a) shows the correlated response, which fully takes into account the final state interaction between the

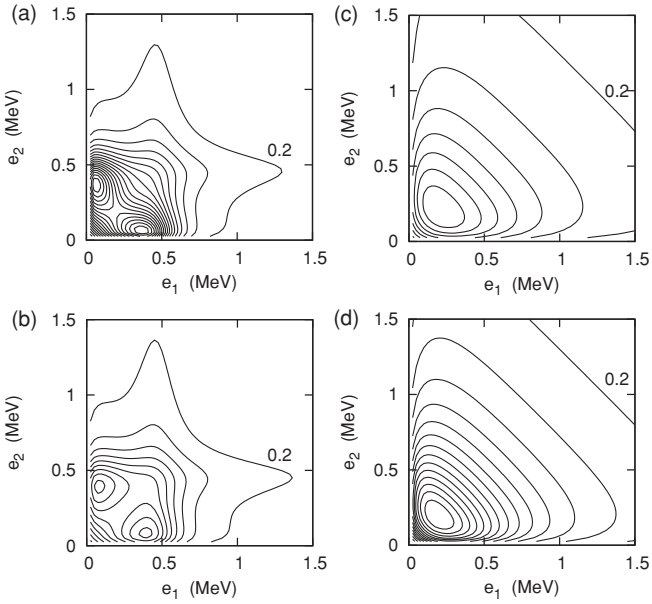

FIG. 1. The dipole strength distributions, $d^2B(E1)/de_1de_2$, of ^{11}Li as a function of the energies of the two emitted neutrons relative to the core nucleus. They are plotted in units of e^2 fm^2/MeV^2. Panel (a) shows the correlated response, which fully takes into account the final state interaction between the two neutrons, while panel (b) shows the unperturbed response, obtained by neglecting the neutron-neutron interaction in the final states. Panels (c) and (d) are obtained by neglecting the neutron-core interaction, without and with the final state interaction between the two neutrons, respectively. The difference between neighboring contour levels is 0.2 e^2 fm^2/MeV^2 for panels (a) and (b), while it is 0.1 e^2 fm^2/MeV^2 for panels (c) and (d).

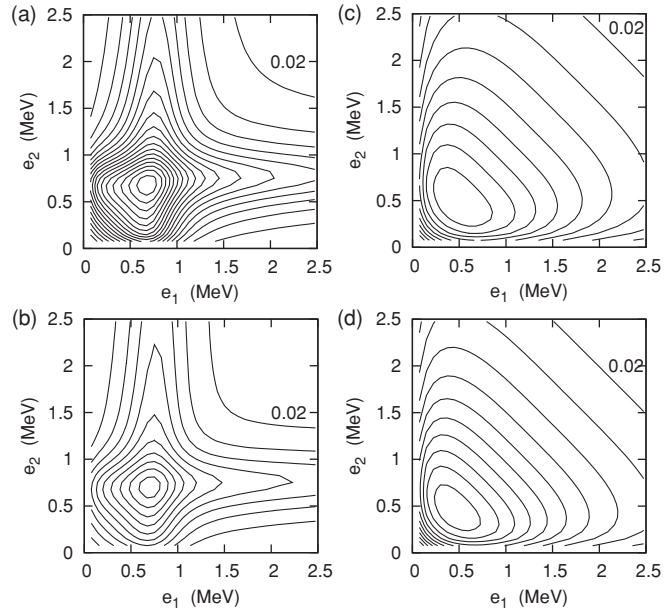

FIG. 2. Same as Fig. 1, but for ^{6}He. The difference between neighboring contour levels is 0.02 e^2 fm^2/MeV^2 for Figs. 2(a) and 2(b), while it is 0.005 and 0.01 e^2 fm^2/MeV^2 for Figs. 2(c) and 2(d), respectively.

two neutrons, while Fig. 1(b) shows the unperturbed response, obtained by neglecting the neutron-neutron interaction in the final states. Figures 1(c) and 1(d) are obtained by neglecting the neutron-core interaction, without and with the final state interaction between the two neutrons, respectively. Figures 2(a)–2(d) are the same as for described for Fig. 1, but for ^{6}He. All the calculations are performed by using the Green's function method [17].

One immediately notices that the strength distribution is considerably different between ^{11}Li and ^{6}He. For ^{11}Li, a large concentration of the strength appears at about $e_1 = 0.375$ MeV and $e_2 = 0.075$ MeV (and at $e_1 = 0.075$ MeV and $e_2 = 0.375$ MeV), with a small ridge at an energy of about 0.5 MeV. However, for ^{6}He, the strength is largely concentrated around $e_1 = e_2 = 0.7$ MeV and a large ridge at about 0.7 MeV appears for both e_1 and e_2 axes. These features remain the same even if the final state interaction between the two emitted neutrons is switched off, as shown in Figs. 1(b) and 2(b), although the degree of the concentration of the strength is much more emphasized by the final state interaction. In contrast, if the interaction between the neutron and the core nucleus is neglected, the strength distribution is altered drastically, and in fact the distribution is now similar between the two nuclei [see Figs. 1(c), 1(d), 2(c), and 2(d)]. Therefore, the different behaviors in the strength distribution should reflect primarily the property of the neutron-core interaction. In fact, the comparisons between Figs. 1(a) and 1(b), 1(c) and 1(d), 2(a) and 2(b), and 2(c) and 2(d) indicate that the final state neutron-neutron interaction does not play a major role in the *shape* of the energy distribution, even though the absolute values are altered.

The ridges in the strength function have already been discussed in the previous calculation for ^{11}Li by Esbensen and Bertsch [17]. They reflect the single-particle resonances, that is, the $p_{1/2}$ resonance around 0.54 MeV for ^{10}Li and the $p_{3/2}$ resonance at 0.91 MeV for ^{5}He [20]. These ridges correspond to the physical process in which one of the neutrons is excited by the dipole field while the other remains near the resonance state as a spectator in the neutron-core system [8,17]. A new finding in the present calculations is the strong two peaks in the two-dimensional energy distributions of ^{11}Li, which is not seen in the case of ^{6}He. That is, for ^{11}Li, in addition to the ridge, the dipole strength is concentrated in the region in which one of the neutrons has an energy close to zero. This reflects the s-wave virtual state in ^{11}Li close to zero energy [18,20,23,24]. This virtual state is characterized by a large negative scattering length of $a = -30^{+12}_{-31}$ fm [13] for the $n + ^9$Li system. In contrast, the s-wave scattering length is $a = 4.97 \pm 0.12$ fm [25] for the $n + ^4$He system, and the virtual state does not exist in ^{5}He. The virtual state in ^{11}Li is taken into account in our calculation by deepening the single-particle potential for even partial waves, as has been done in Refs. [20,24]. Notice that the virtual state was not taken into account in the previous calculation for the dipole response of ^{11}Li in Ref. [17], and the concentration of the strength in the region of $e_1 \sim 0$ and $e_2 \sim 0.4$ MeV was not found there.

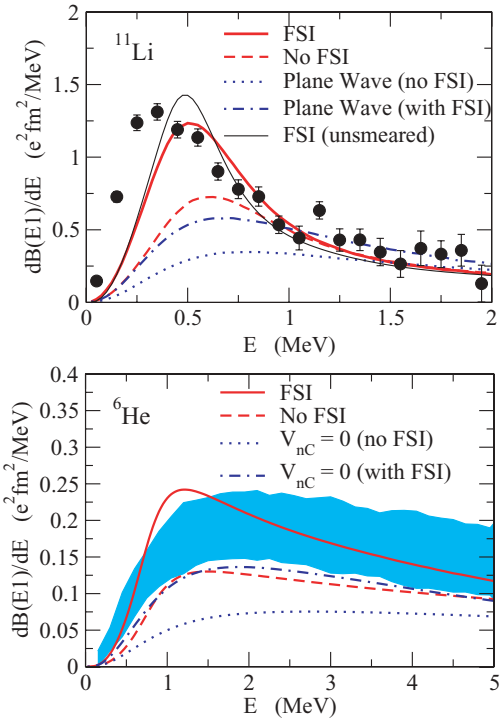

FIG. 3. (Color online) (Top) The dipole strength distribution for ^{11}Li as a function of $E = e_1 + e_2$. The thick solid, dashed, dotted, and dot-dashed lines were obtained under the same assumptions as for Figs. 1(a), 1(b), 1(c), and 1(d), respectively. These curves are smeared with the experimental energy resolution. The thin solid line is the same as the thick solid line, but without the smearing. The experimental data are taken from Ref. [6]. (Bottom) The same as the top panel, but for ^{6}He. The shaded area shows the experimental data, taken from Ref. [7].

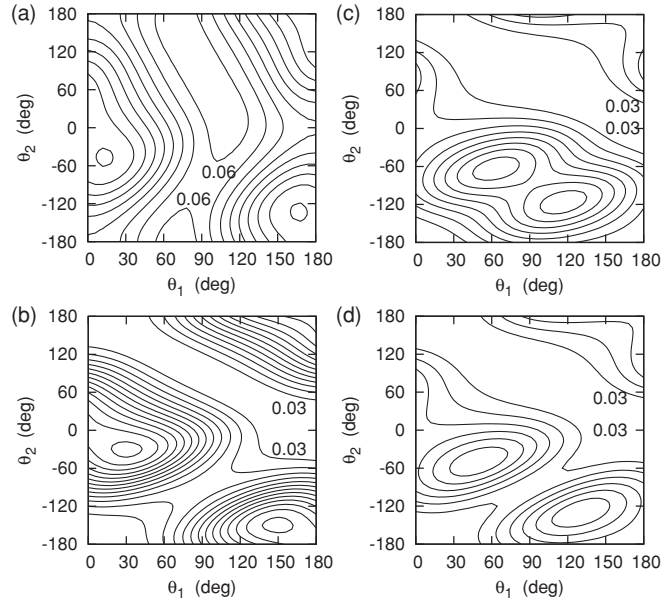

FIG. 4. Angular distributions of the two valence neutrons in ^{11}Li and ^{6}He emitted in the rest frame of the corresponding nuclei. These are calculated for the configuration in which the two neutrons are emitted in the same reaction plane (i.e., $\phi_1 = \phi_2$) by the longitudinal component of the $E1$ operator. Panel (a) shows the angular distribution for ^{11}Li at $e_1 = 0.375$ MeV and $e_2 = 0.075$ MeV, while panels (b) and (c) are for $e_1 = e_2 = 0.225$ MeV and $e_1 = e_2 = 0.5$ MeV, respectively. Panel (d) shows the angular distribution for ^{6}He at $e_1 = e_2 = 0.7$ MeV. The difference between neighboring contour levels is 0.03.

It has been argued that the two-peaked structure in the energy distribution is a characteristic feature of the Efimov effect [18]. However, the s-wave scattering length in our calculation is -5.6 fm [9,20], whose magnitude is much smaller than the empirical value. It is therefore not obvious whether the energy distribution for ^{11}Li can be interpreted in terms of the Efimov effect, and further theoretical studies will be needed to clarify this point.

The dipole strength distributions,

$$\frac{dB(E1)}{dE} = \int de_1 de_2 \, \frac{d^2B(E1)}{de_1 de_2} \, \delta(E - e_1 - e_2), \qquad (1)$$

are plotted in Fig. 3. The solid, dashed, dotted, and dot-dashed lines were obtained under the same assumptions for Figs. 1(a)/2(a), 1(b)/2(b), 1(c)/2(c), and 1(d)/2(d), respectively. These curves are smeared with the experimental energy resolution [6]. The thin solid line in Fig. 3(a) is the same as the thick solid line, but without the smearing. Notice that the discretized dipole strength function has been computed in Ref. [21], in which the strength function was smeared with a phenomenological width. In contrast, in Fig. 3, the dipole strength is calculated using the continuum scattering wave functions, and the energy smearing is automatically taken into account except for the experimental energy resolution.

The experimental $B(E1)$ distribution for ^{11}Li is obtained from the experimental breakup cross sections in Ref. [6], using $S_{2n} = 378$ keV. Because of the large concentration of the strength in the low energy region in the energy distribution shown in Fig. 1, the strength distribution for ^{11}Li has a significantly sharper peak as compared to that for ^{6}He. Notice again that the strength distributions are qualitatively similar between the two nuclei if the neutron-core potential is neglected (see the dotted and the dot-dashed lines).

To discuss how the dineutron correlation in the ground state affects the dipole response, let us next consider the angular distributions of the two emitted neutrons. Figure 4 shows the angular distributions corresponding to the longitudinal component of the dipole excitation of the ^{11}Li and ^{6}He nuclei (induced by the $\mu = 0$ component of the $E1$ operator, $\hat{T}_{\lambda=1,\mu=0}$), that is, $\sum_{h_1,h_2} |f^{10}_{h_1h_2}(\hat{\boldsymbol{k}}_1, \hat{\boldsymbol{k}}_2)|^2$, where h and $\hat{\boldsymbol{k}} = (\theta, \phi)$ are the helicity and the direction of the momentum vector for an emitted neutron, respectively. Here, $f^{1\mu}_{h_1h_2}(\hat{\boldsymbol{k}}_1, \hat{\boldsymbol{k}}_2)$ is the amplitude of dipole excitation calculated with two-particle wave functions in the continuum state with definite momenta $\boldsymbol{k}_1$ and $\boldsymbol{k}_2$ and definite spins, where the momenta are defined in the rest frame of ^{11}Li and ^{6}He (see Eq. (5.5) in Ref. [17]). Notice that the angular distributions for the $\mu = \pm 1$ components are identical

to those for the $\mu = 0$ component, when they are rotated by 90 degrees [17].

The angular distribution for ^{11}Li at the energy at which the dipole strength is concentrated, that is, $e_1 = 0.375$ MeV and $e_2 = 0.075$ MeV (see Fig. 1), is shown in Fig.4(a). The distribution is calculated for the configurations in which the two emitted neutrons are in the same reaction plane, that is, $\phi_1 = \phi_2$. Here the second neutron mainly occupies the s-wave virtual state, and the angular distribution for this neutron is widely spread. The energy and angular distributions are mainly determined by the virtual state for this energy configuration, and the effect of final state interaction does not seem to play a major role, as one can infer from Fig. 1. We have confirmed this by switching off the final state interaction in our calculation. We have in fact obtained an angular distribution qualitatively similar to that in Fig. 4(a).

The angular distribution for the same total energy $e_1 + e_2 = 0.45$ MeV as in Fig. 4(a), but for $e_1 = e_2 = 0.225$ MeV, is plotted in Fig. 4(b). For this configuration, both the neutrons are emitted along the z axis (i.e., $\theta_1 = \theta_2 = 0$) with a large probability, although the distribution is rather flat around $\theta_1 = \theta_2 = 0$, with the maximum at $\theta_1 = -\theta_2 = 30^\circ$. Therefore, the opening angle between the two neutrons is relatively small, and one would naively consider that the shape of this distribution strongly reflects the dineutron correlation, with some perturbation by the anticorrelation effect for the dipole excitation.

The anticorrelation is more pronounced at higher energies. Figure 4(c) shows the angular distribution at $e_1 = e_2 = 0.5$ MeV, which corresponds to the region of the ridge in the energy distribution shown in Fig. 1. For this energy configuration, the probability for emission of two neutrons on the same sides of the z axis (in the region of $\theta_2 > 0$) is largely suppressed, and the maximum of the distribution appears around $\theta_1 = 60^\circ$ and $\theta_2 = -66^\circ$. Notice that the shape of the distribution is similar to the results of the previous calculation shown in Figs. 9 and 10 in Ref. [17]. The shape is determined by a destructive interference between the $[d \otimes p]$ and $[p \otimes s]$ configurations [17], excited from the $[p^2]$ and $[s^2]$ configurations in the ground state wave function. Therefore, the angular distribution around this energy is strongly affected by the p-wave single-particle resonance. In fact, for the ^{6}He nucleus, where the energy distribution is characterized by the $p_{3/2}$ resonance, we obtain a very similar angular distribution at $e_1 = e_2 = 0.7$ MeV [see Fig. 4(d)]. For ^{6}He, it would therefore not be straightforward to probe the dineutron correlation in the ground state solely by the angular distribution, in which the dineutron correlation is largely masked by the effect of the p-wave single-particle resonance.

In summary, we studied the energy and angular distributions of the two emitted neutrons from $E1$ excitations in ^{11}Li and ^{6}He using the three-body model. We have shown that the two-dimensional energy distributions for ^{11}Li have a two-peaked structure, whereas those for ^{6}He have one single peak. This difference originates from the existence of a virtual s state in the residual ^{10}Li nucleus, while no virtual state exists in ^{5}He. Thus, these distributions are strongly affected by the neutron-core potential and the s-wave mixing probability in the ground states. This is in a marked contrast with the geometry of the Borromean nuclei, where the neutron-neutron interaction plays an essential role in emerging the strong dineutron correlation. For the ^{11}Li nucleus, under the presence of the s-wave virtual state, a clear manifestation of the strong dineutron correlation can be seen through the angular distributions of the two emitted neutrons. For the ^{6}He nucleus, however, the anticorrelation effect dominates in the angular distribution and it is not straightforward to probe the di-neutron correlations in it. The correlation measurements for ^{11}Li have been recently done at RIKEN. The present calculations shown in this article are in good agreement with the preliminary data. A more detailed analysis of the experimental data will be reported soon.

We thank P. Schuck for useful discussions. This work was supported by the Japanese Ministry of Education, Culture, Sports, Science and Technology by a Grant-in-Aid for Scientific Research under the Program Numbers (C) 19740115 and 20540277.

[1] M. V. Zhukov *et al.*, Phys. Rep. **231**, 151 (1993).
[2] A. S. Jensen *et al.*, Rev. Mod. Phys. **76**, 215 (2004).
[3] C. Bachelet *et al.*, Phys. Rev. Lett. **100**, 182501 (2008).
[4] I. Tanihata *et al.*, Phys. Rev. Lett. **55**, 2676 (1985).
[5] P. G. Hansen and B. Jonson, Europhys. Lett. **4**, 409 (1987).
[6] T. Nakamura *et al.*, Phys. Rev. Lett. **96**, 252502 (2006).
[7] T. Aumann *et al.*, Phys. Rev. C **59**, 1252 (1999).
[8] G. F. Bertsch and H. Esbensen, Ann. Phys. (NY) **209**, 327 (1991).
[9] K. Hagino and H. Sagawa, Phys. Rev. C **72**, 044321 (2005).
[10] K. Hagino, H. Sagawa, J. Carbonell, and P. Schuck, Phys. Rev. Lett. **99**, 022506 (2007).
[11] M. Matsuo, K. Mizuyama, and Y. Serizawa, Phys. Rev. C **71**, 064326 (2005).
[12] N. Pillet, N. Sandulescu, and P. Schuck, Phys. Rev. C **76**, 024310 (2007).
[13] H. Simon *et al.*, Nucl. Phys. **A791**, 267 (2007); Few-Body Syst. **43**, 199 (2008).
[14] L. V. Chulkov *et al.*, Nucl. Phys. **A759**, 23 (2005).
[15] B. V. Danilin *et al.*, Phys. Rev. C **73**, 054002 (2006).
[16] F. M. Marqués *et al.*, Phys. Rev. C **64**, 061301(R) (2001).
[17] H. Esbensen and G. F. Bertsch, Nucl. Phys. **A542**, 310 (1992).
[18] E. Garrido, D. V. Fedorov, and A. S. Jensen, Phys. Rev. Lett. **96**, 112501 (2006).
[19] V. M. Efimov, Phys. Lett. **B33**, 563 (1970).
[20] H. Esbensen, G. F. Bertsch, and K. Hencken, Phys. Rev. C **56**, 3054 (1997).
[21] K. Hagino and H. Sagawa, Phys. Rev. C **76**, 047302 (2007).
[22] H. Esbensen, K. Hagino, P. Mueller, and H. Sagawa, Phys. Rev. C **76**, 024302 (2007).
[23] B. M. Young *et al.*, Phys. Rev. C **49**, 279 (1994).
[24] I. J. Thompson and M. V. Zhukov, Phys. Rev. C **49**, 1904 (1994).
[25] R. A. Arndt *et al.*, Nucl. Phys. **A209**, 429 (1973).